Comptes Rendus

Chimie

Haining Li, Tiantian Zhang, Kai Tang, Binglin Li, Xiaoli Zhang, Binxia Zhao and Jiao Wang

Preparation of hyperbranched 4-dimethylaminopyridine catalyst for the efficient synthesis of vitamin E succinate

Full paper / *Article*

Preparation of hyperbranched 4-dimethylaminopyridine catalyst for the efficient synthesis of vitamin E succinate

Haining Li[#, *a*]**, Tiantian Zhang**[#, *a*]**, Kai Tang**[*b*]**, Binglin Li**[® *a*]**, Xiaoli Zhang**[® *, a*]**, Binxia Zhao**[*b*] **and Jiao Wang**[*, c*]

[*a*] College of Food Science and Engineering, Northwest University, Xi'an, Shaanxi 710000, China

[*b*] School of Chemical Engineering, Northwest University, Xi'an, Shaanxi 710000, China

[*c*] BioQuant, Heidelberg University, Heidelberg, 69120, Germany

E-mails: 824818830@qq.com (H. Li), zhangttbetter@126.com (T. Zhang), 745621535@qq.com (K. Tang), libinglin@nwu.edu.cn (B. Li), xlzhang@nwu.edu.cn (X. Zhang), zhaobx@nwu.edu.cn (B. Zhao), jiao.wang@bioquant.uni-heidelberg.de (J. Wang)

Abstract. Sorbitol was employed as the grafting agent to modify nano-silica by the hyperbranched reaction. The obtained carrier was further used to prepare immobilized 4-dimethylaminopyridine (DMAP), which was successfully applied to produce vitamin E succinate. Two crucial steps were systematically investigated during the preparation of hyperbranched loaded DMAP: the epoxy-alcohol addition and N-alkylation reactions. For the epoxy-alcohol addition reaction, the maximum hydroxyl content reached 8.89 mmol/g when the molar ratio of sorbitol to epoxide was 2.5:1, the reaction temperature was 55 °C, the stirring rate was 500 rpm, and the reaction time was 8 h. In the N-alkylation reaction, when the reaction time was 20 h, the reaction temperature was 130 °C, the molar ratio of MAP to K_2CO_3 was 1:1.5, the KI to MAP molar ratio was 1:1 and the stirring rate was 600 rpm, the highest loading of DMAP reached 5.17 mmol/g. The catalytic performance of the loaded DMAP with different branching levels was evaluated by the acetylation reaction. The highest catalytic activity was observed in the hyperbranched catalyst, which reached 24.97 mmol/h·g. Moreover, the stability of the prepared immobilized DMAP was significantly enhanced. After being used for ten batches, 94.9% of the catalytic activity retention rate was obtained.

Keywords. Sorbitol, Nano silica, Hyperbranched, DMAP, Acylation reaction, Vitamin E succinate.

Manuscript received 25 August 2022, revised 1 November 2022, accepted 22 November 2022.

---

[*] Corresponding authors.

[#] Contributed equally.

1. Introduction

4-dimethylaminopyridine (DMAP) is a classical super nucleophilic acylation catalyst that can catalyze acylation, alkylation, etherification, esterification, and ester exchange reactions. Therefore, DMAP is widely used in organic synthesis, drug synthesis, dyestuff, fragrance, polymer chemistry, and analytical chemistry [1,2]. However, as a homogeneous catalyst, it's tough to separate DMAP from the reaction system, which pollutes the following product. Therefore, immobilization should be a requisite for commercial applications of DMAP since immobilization permits the easy recycling of catalysts and simplifies the design and performance control of the reactors.

Researchers found that inorganic silica-based carriers with large specific surface areas, active hydroxyl groups, and excellent mechanical properties are excellent choices for carriers to prepare the immobilized catalysts [3,4]. Therefore, nano-silica (NS) was chosen as the carrier for the immobilization of DMAP in this paper. Because of nano silica's sizeable specific surface area, high porosity, and many surface active centers, nano silica has potential applications in catalysts and catalyst carriers. However, the hydroxyl content on the surface of NS is not very high, which limits the scope of active components for its coupling, so the loading of the prepared immobilized catalysts is correspondingly low. Fortunately, by introducing the concept of hyperbranched polymers, it was demonstrated that they possess even more superior properties [5]. Hyperbranched polymers are a class of highly branched macromolecules with many branching points and less tangled molecular chains. And a viscosity that does not change with increasing molecular weight. And more large terminal functional groups can be easily modified to synthesize various available materials [6–8]. Moreover, the reaction of polyhydroxy compounds with modified silica gel could generate polyhydroxy silica gel to increase the surface hydroxyl content of silica gel. So, it is crucial to select suitable polyhydroxy compounds as branching agents. Since sorbitol has six hydroxyl groups, it has great promise in increasing the hydroxyl content of the NS surface. Therefore, in this thesis, sorbitol was finally selected as the grafting agent and nano-silica as the carrier, and sorbitol was grafted onto the carrier surface by hyperbranched technique to achieve a more

significant expansion of the hydroxyl content on the surface of nano-silica, resulting in a higher loading of hyperbranched polymer DMAP. The hyperbranched polymer DMAP dramatically reduces the production cost and makes the preparation process greener and safer by using KI to facilitate the N-alkylation reaction and avoid the hazardous chemical NaH.

Vitamin E Succinate (VES) is a derivative of vitamin E. Studies have confirmed that VES not only inhibits the growth of tumor cells but also induces apoptosis [9–17]. More exciting is that VES is not toxic to normal cells and has no growth inhibitory effect, demonstrating the importance and broadness of VES application prospects in the medical field. VES is usually prepared in the presence of a basic catalyst, and the acidic catalyst will darken the product [18–20]. The basic catalysts are sodium acetate, potassium carbonate, pyridine, tertiary amines, etc. Among them, DMAP as a catalyst eliminates the possible emulsification during the preparation process and improves the yield of VES [21]. Therefore, to synthesize VES more efficiently, vitamin E and succinic anhydride were chosen as reactants, and appropriate amounts of hyperbranched-loaded DMAP catalysts were used for the catalytic synthesis of VES. The experimental results showed that the hyperbranched-loaded DMAP offered excellent catalytic performance and further demonstrated the successful preparation of the hyperbranched-loaded DMAP catalyst.

2. Materials and methods

2.1. *Materials*

Nano-silica (NS) was purchased from Qingdao Ocean Chemical Co., Ltd. KH-560 (γ-glycidyl ether isopropyl trimethylsilyl) was purchased from Hangzhou Jessica Chemical Co., Ltd. 4-methylaminopyridine (MAP) and Succinic anhydride were all from Aladdin Reagent Co., Ltd. Vitamin E, sorbitol, and epichlorohydrin (epichlorohydrin) were purchased from Sinopharm Group. The rest of the relevant reagents, including the salts used, were purchased by the laboratory following the standards.

2.2. *Preparation of unbranched NS-loaded DMAP catalysts*

Firstly, a certain amount of NS, anhydrous ethanol, and deionized water was mixed into a round bottom flask, and then a quantitative amount of 3-chloropropyltrimethoxysilane was added. After the reaction was completed, the resulting intermediate NS-Cl was treated and subjected to N-alkylation with MAP to produce a non-branched NS-loaded catalyst.

2.3. *Preparation of grafted NS-loaded DMAP catalysts*

The silyl carriers were modified in the first step by coupling reaction using KH-560 [22–24]. In the second step, the epoxide group of the epoxidized carriers was reacted with the hydroxyl group in sorbitol by employing an epoxy-alcohol addition reaction to obtain Intermediate 1: polyhydroxyal carriers. In the third step, the intermediate polyhydroxy carriers were modified with epichlorohydrin to synthesize middle 2: polychlorinated carriers. In the fourth step, DMAP loading was carried out by the N-alkylation technique, i.e., the polychlorinated carriers reacted with the precursor MAP to produce the branching NS-loaded DMAP catalyst.

2.4. *Preparation of hyperbranched NS-loaded DMAP catalysts*

Nano-silica was chosen as the carrier, sorbitol as the branching agent, and MAP was combined to synthesize the hyperbranched loaded DMAP catalyst. The specific route is shown in Figure 1: In the first step, the nano-silica carrier was modified by coupling with KH-560. The reaction was carried out at 95 °C for 18 h. After centrifugation, the residue was washed and dried under a vacuum at 60 °C to obtain the epoxy-functionalized silica nanocarrier. In the second step, the epoxy group was then used to produce polyhydroxy nano-silica with sorbitol utilizing an epoxy-alcohol addition reaction. Namely, 30 mL of DMF and epoxidized nano-silica carriers were added to a 250 mL three-neck flask, stirred, and then drafted with sorbitol. 50 µL of BF_3-$C_2H_5OC_2H_5$ solution was added at a fixed interval of 1 h during the reaction for catalysis. After centrifugation, the residue was washed and dried in a vacuum at 60 °C to obtain a polyhydroxy-functionalized silica-based carrier. In the third step, the poly hydroxylated silica nanocarriers were modified with KH-560 to get hyperbranched epoxidized silica nanocarriers. The reaction was carried out at 95 °C for 18 h. After centrifugation, the residue was washed and dried under a vacuum at 60 °C to obtain a super-branched epoxy-functionalized silica carrier. In the fourth step, the hyperbranched epoxidized carriers were then drafted with sorbitol to bring hyperbranched polyhydroxy silica carriers. That is, 30 mL of DMF and the super branched epoxy-functionalized nano-silica carrier were added successively to a 250 mL three-neck flask, stirred, and then drafted with sorbitol. During the reaction, 50 µL of BF_3-$C_2H_5OC_2H_5$ solution was added at fixed intervals for 1 h to catalyze the reaction. After completion, the precipitate was centrifuged, washed, and dried under vacuum at 60 °C to obtain a superb ranched polyhydroxy-functionalized silica-based carrier. In the fifth step, the hyperbranched polyhydroxy carriers were modified with epichlorohydrin to get hyperbranched polyalkylchlorosilyl carriers. That is: add 30 mL of N, N-dimethylformamide solvent, and the polyhydroxy silyl carrier produced in the previous step to a 250 mL three-necked flask, stir thoroughly and then add epichlorohydrin precisely with a pipette. During the reaction, for catalysis, 50 µL of BF_3-$C_2H_5OC_2H_5$ solution was added at fixed intervals of 1 h. After centrifugation and subsequent washing of the residue at the end of the reaction, the nano-silica carriers were dried under vacuum at 60 °C to obtain stacked grafted polychlorinated functionalized silica carriers. In the sixth step, the precursor MAP was used to carry out the N-chloroalkylation reaction with the prepared polychlorinated spherical silica to obtain the target catalyst. The reaction was carried out by adding 25 mL of o-xylene to the weighed MAP in a microreactor, mixing and dissolving, then adding K_2CO_3, KI, and the hyperbranched polychlorinated functionalized nano-silica carrier from the previous step, and protecting the reaction with nitrogen for 24 h. Samples were taken at 2 h intervals, 50 µL each time. After termination of the reaction, the target catalyst was repeatedly washed, and the resulting wash solution was analyzed to determine the amount of MAP in the total wash solution to obtain the hyperbranched loaded DMAP.
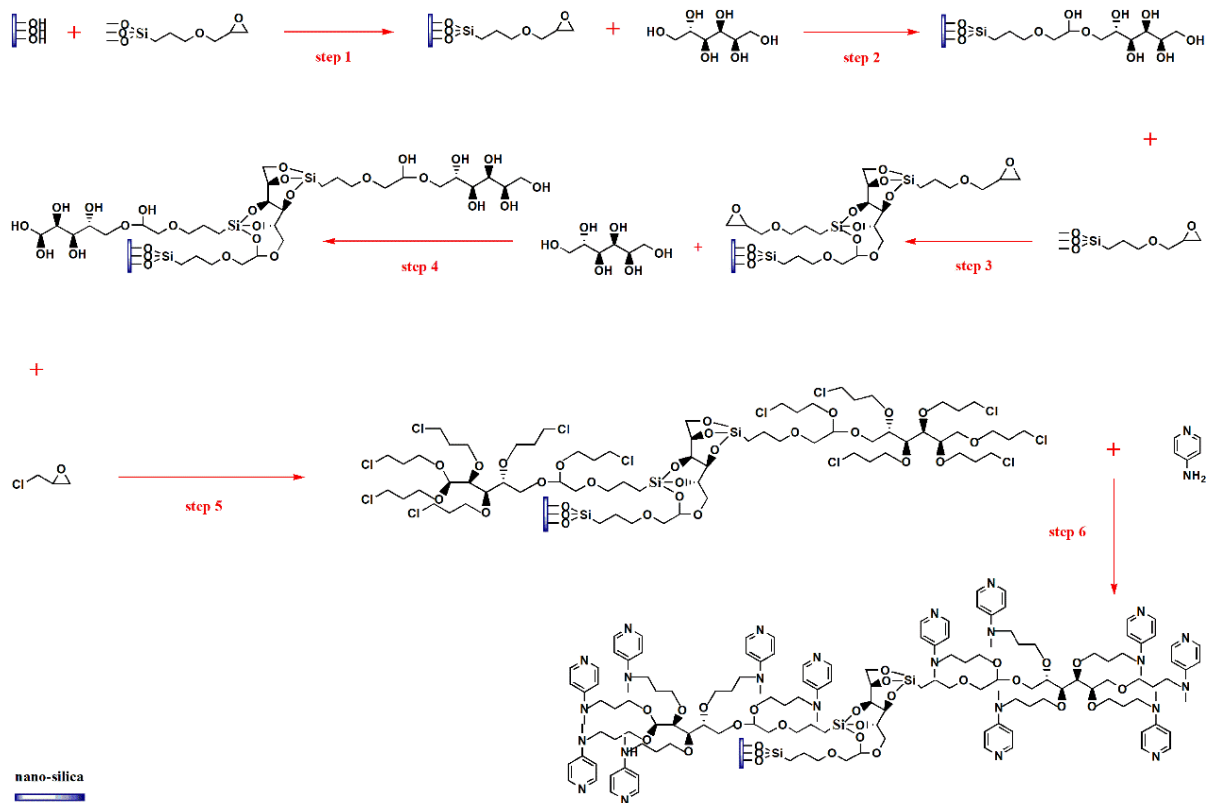
Figure 1. Preparation of hyperbranched NS-loaded DMAP catalysts.

2.5. *Determination of branching-loaded DMAP loadings*

The loading of the target catalyst was calculated by the difference between the initial MAP concentration in the system after the input of the precursor MAP and the residual MAP concentration in the system after the termination of the reaction. In contrast, the TLC method determined the MAP concentration in the reaction [25,26]. After a series of experimental operations through the preparation of the unfolding agent, capillary spotting, plate walking, color development, and scanning of the pictures, the pictures were processed with the help of Photoshop and Gel-Pro. The images were processed with software such as Photoshop and Gel-Pro analyzer, and the spots were converted into corresponding grey-scale data, which was then used to calculate the amount of MAP. The concentration of MAP remaining after the termination of the reaction was determined.

2.6. *The process of acylation of vitamin E*

After adding vitamin E and acetic anhydride to the microreactor, 5 mL of toluene was added to dissolve the reaction. Finally, the super branching-loaded DMAP catalyst was added, and the reaction was carried out at 60 °C for 12 h at 600 rpm. In addition, 60 μL of the reaction mixture was pipette at the initial and termination stages of the reaction, respectively, and centrifuged at 3000 rpm for 4 min in a low-speed centrifuge. After centrifugation, 30 μL of the supernatant was taken separately, and the amount of vitamin E was measured by HPLC.

2.7. *Synthesis of vitamin E succinate*

After adding 0.5 mmol of vitamin E to the microreactor, 5 mL of toluene was added and stirred until it dissolved. Then 1.5 mmol of succinic anhydride was added, and then hyperbranched loaded DMAP catalyst and free DMAP catalyst were added to the reactor.

The reaction was carried out for 12 h at 500 rpm and 55 °C under nitrogen protection. The conversion rate of vitamin E was calculated after the reaction was terminated.

2.8. *High-performance liquid chromatography analysis*

The amount of vitamin E in the reaction system was determined by high-performance liquid chromatography. The detection conditions were as follows: an Inert Sustain C18 column was used, the column temperature was 40 °C, the mobile phase was glacial acetic acid/methanol (V/V: 3.2/500), and the flow rate was 1 mL/min, and the detection wavelength was 284 nm. Finally, the difference in the content of vitamin E before and after the reaction was used to calculate the conversion of vitamin E.

3. Results and discussion

3.1. *Preparation of loaded DMAP catalysts with different branching degrees*

The preparation of unbranched NS-loaded DMAP catalyst, the practice of branched NS-loaded DMAP catalyst, and the preparation of super branched NS-loaded DMAP catalyst are described in Sections 2.2, 2.3, and 2.4 above. The synthetic route of the final target catalyst prepared therein, the hyperbranched NS-loaded DMAP, is shown in Figure 1 above. By analyzing the steps of the artificial course, the reaction conditions related to the epoxy-alcohol addition reaction in the fourth step and the N-alkylation reaction process in the sixth step were explored as the focus of this paper.

3.2. *Optimization of epoxy-alcohol addition reaction conditions*

3.2.1. *Effect of molar ratio on the hydroxyl content of and eventually*

As shown in Figure 2, the hydroxyl content was significantly increased with the increasing dendrimer (sorbitol) molar ratio to an epoxy group. When the dendrimer to epoxy group ratio reached 2.5:1, the hydroxyl content reached the maximum value of 7.85 mmol/g. After that, with the increasing molar
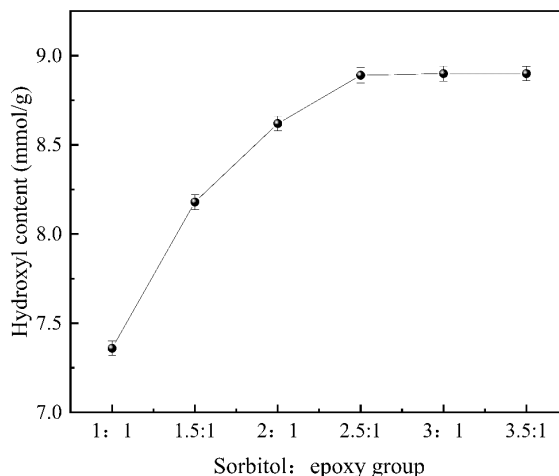
Figure 2. The influences of molar ratio on hydroxyl content.

ratio of the dendrimer and epoxy group, the mass transfer resistance of the system was also increased, so the hydroxyl content no longer changed significantly. Moreover, increased dendrimer and epoxy group inputs adversely affected the subsequent product separation and purification and wasted raw materials. Therefore, the optimal molar ratio of the dendrimer to the epoxy group was 2.5:1 on all considerations.

3.2.2. *Effect of reaction temperature on the final hydroxyl content*

As shown in Figure 3, the hydroxyl content increased as the reaction temperature increased, and when the reaction temperature reached 55 °C, the hydroxyl content was 8.35 mmol/g. After that, there was no significant change in the hydroxyl content when the temperature continued to increase. It is because, at the beginning of the reaction, the adequate number of collisions is insufficient due to the low temperature, which makes the reaction occur slowly, and the hydroxyl content is relatively low. As the temperature continues to increase, the number of effective collisions occurring in the reaction increases, the chance of addition reaction increases, the reaction rate accelerates, and the hydroxyl content increases. However, after the temperature exceeded 55 °C, the number of effective collisions reached the maximum, the hydroxyl content stopped changing, and the high temperature was a kind of loss and waste to the
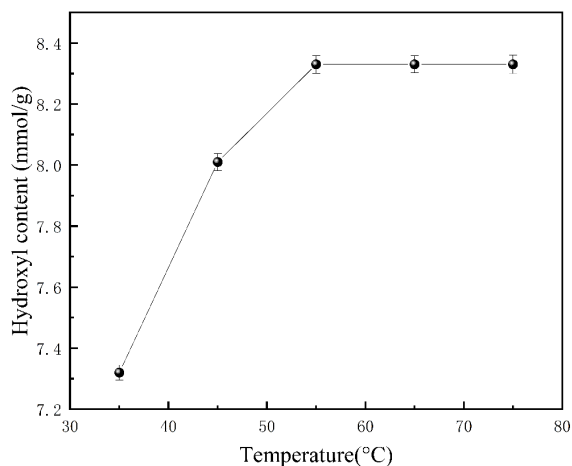
Figure 3. The influences of reaction temperature on hydroxyl content.

Figure 4. The influences of stirring speed on hydroxyl content.

instrument and energy. Therefore, the best reaction temperature is 55 °C.

3.2.3. *Effect of stirring rate on the final hydroxyl content*

As shown in Figure 4, with the increase in stirring rate, the reaction rate of the system increased, and the hydroxyl content also increased accordingly. When the stirring rate reached 500 rpm, the reaction rate reached the maximum, and the hydroxyl content increased to 8.89 mmol/g. However, after the moving rate exceeded 500 rpm, there was almost no significant change in the reaction rate, so the hydroxyl content remained virtually the same. It is because at the initial stirring speed of 300 rpm, due to insufficient stirring, most of the input reaction materials were at the bottom of the reaction vessel. The reaction materials were not wholly contacted with the dendrimer due to the influence of the mass transfer resistance of the system, resulting in a slow reaction, and the hydroxyl content was relatively small. As the stirring rate increases, the mass transfer resistance decreases, and the contact between the branching agent and the epoxy group becomes adequate. The reaction rate also increased, and the hydroxyl content also increased accordingly. When the stirring rate reached 500 rpm, the hydroxyl content reached the maximum. However, when the moving speed is further increased, the hydroxyl content is no longer changed after reducing the mass transfer resistance
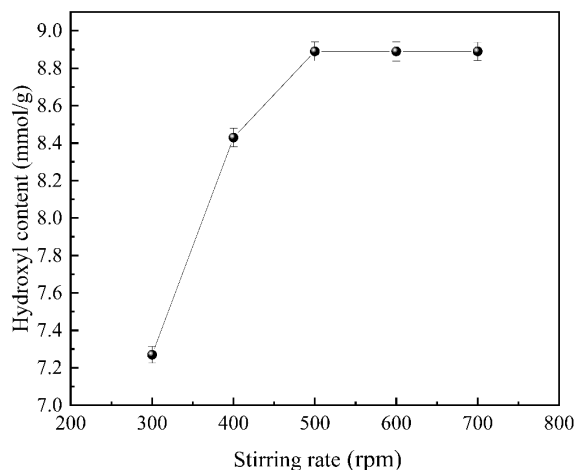
to a certain extent, and energy is consumed. Therefore, the optimum stirring rate for the reaction is 500 rpm.

3.2.4. *Effect of reaction time on the final hydroxyl content*

As shown in Figure 5, with the extension of the reaction time, the hydroxyl content in the system was obviously on a rising trend. Still, when the reaction proceeded to 8 h, the hydroxyl content reached 8.89 mmol/g, and after that, the hydroxyl content did not increase significantly by further extending the reaction time. It may be because when the density of the branching agent reaches a specific range, the hydroxyl groups are closely arranged on the surface of nano silica. At this time, sorbitol is no longer so easy to diffuse to the reaction site, and the hydroxyl content will not change with time; accordingly, the continued extension of time also consumes energy and increases the cost. Hence, the optimal reaction time is 8 h.

3.3. *Optimization of process conditions for DMAP loading reactions*

3.3.1. *Effect of reaction time on DMAP loading*

As shown in Figure 6, the loading of DMAP increased significantly with the gradual increase of the reaction time. When the reaction proceeded to
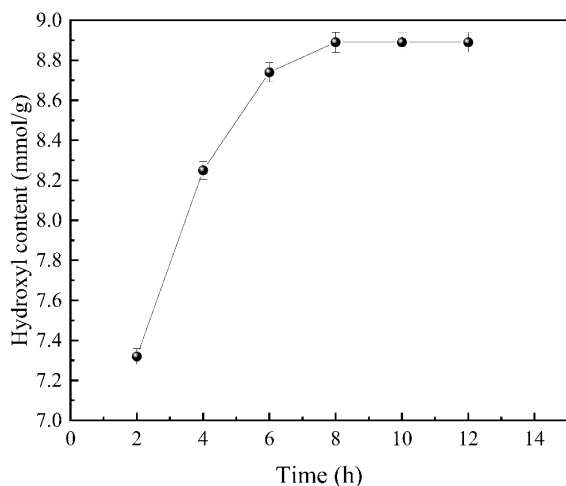
Figure 5. The influences of reaction time on hydroxyl content.

Figure 6. The influences of reaction time on catalyst loading.
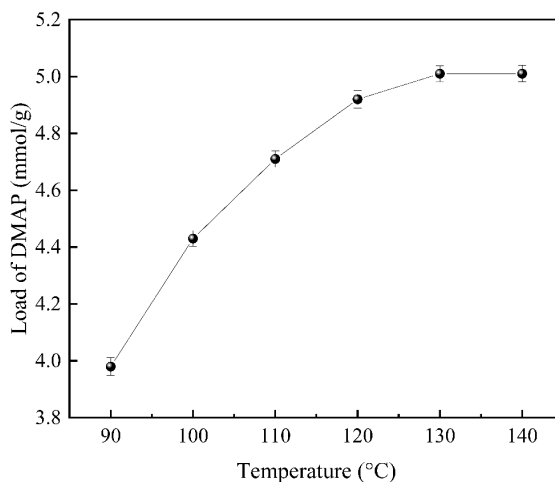
Figure 7. The influences of reaction temperature on DMAP loading.

20 h, the loading of the catalyst was 4.87 mmol/g, after which the loading did not change significantly with the increasing reaction time. It may be because the hyperbranched polychlorinated functionalized nano-silica carrier surface was densely packed with MAP when the reaction proceeded to 20 h. Therefore, when the reaction time was extended beyond 20 h, MAP could not quickly contact the active sites on the carrier surface anymore and wasted energy. Hence, the optimal reaction time was 20 h.

3.3.2. *Effect of reaction temperature on DMAP loading*

As shown in Figure 7, the effect of temperature on the loading was relatively significant. With the increase in reaction temperature, the loading of the DMAP catalyst reached the maximum value of 5.01 mmol/g at 130 °C, after which the loading did not change significantly when the reaction temperature continued to be increased. It is due to the low number of effective collisions at low temperatures, and the reaction occurs more slowly, which lowers the loading amount. With the increase in the reaction temperature, the number of activated molecules increased, and the number of effective collisions increased. Then the reaction rate accelerated, and the loading amount increased accordingly. However, when the reaction temperature exceeds 130 °C, there is no significant change in the loading because the
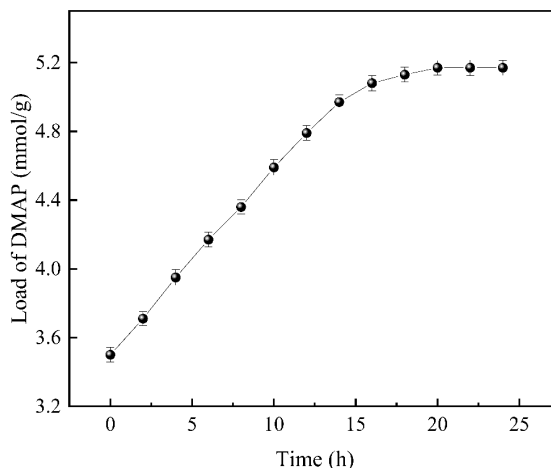
temperature is close to the boiling point of o-xylene (140 °C). O-xylene is the reaction solvent, and sublimation occurs at high temperatures, making the reaction incomplete, thus affecting the purity and yield. Meanwhile, too-high temperatures waste energy and pose safety hazards, so the optimal temperature for this reaction is 130 °C.

3.3.3. *Effect of potassium carbonate input on DMAP loading*

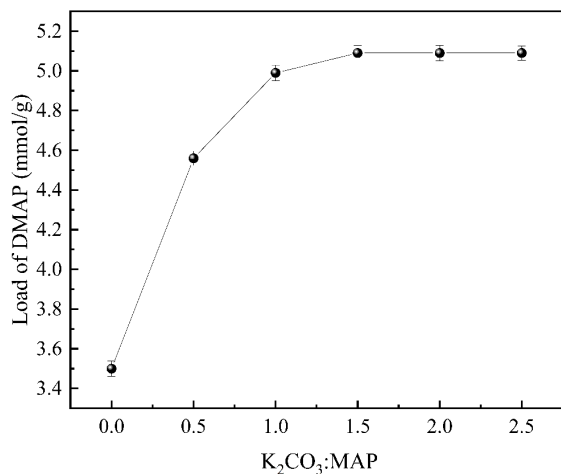Adding K_2CO_3 has a catalytic effect on the N-alkylation reaction and can create a virtual

Figure 8. The effect of potassium carbonate addition on DMAP loading.

Figure 9. The influence of potassium iodide input on DMAP loading.

environment, thus enhancing the onset of loading. As shown in Figure 8, with the increase of K_2CO_3 input, the DMAP loading increased continuously. The catalyst loading reached 5.09 mmol/g when the molar ratio of MAP to K_2CO_3 was 1:1.5. However, when the molar ratio of both exceeded 1:1.5, the loading remained the same. At this time, if potassium carbonate continued to be added to the reaction system, it would make the design too basic, which was not conducive to an adequate reaction. It wastes reagents and increases the cost. Therefore, the amount of K_2CO_3 input should be 1:1.5 for MAP: K_2CO_3.

3.3.4. *Effect of the amount of potassium iodide on the DMAP loading*

KI was added as a catalyst for the N-alkylation reaction to play a catalytic role, thus enhancing the loading of DMAP. As shown in Figure 9, the loading of DMAP increased with the increasing amount of KI input. The DMAP loading reached the maximum value of 5.10 mmol/g when the input amount met the molar ratio of KI to MAP of 1:1. As the reaction proceeded, the input amount of KI continued to increase. When the molar ratio of KI to MAP exceeded 1:1, there was no noticeable change in the loading amount. The reason is that the appropriate amount of catalyst can effectively increase the activation molecule number of the reaction system, which is conducive to improving the reaction rate and thus in-
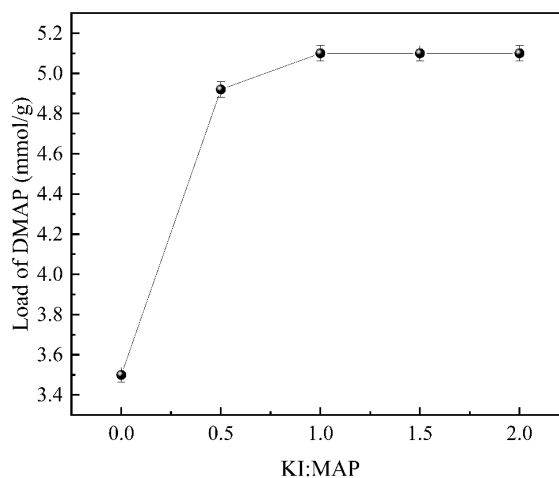
creasing the loading of DMAP. Still, adding excessive catalyst reduces the activation molecule number. It, therefore, produces side effects, which are detrimental to the reaction rate and decrease DMAP Loading, waste the reagent, and increase the cost. Therefore, the amount of KI input is optimal when MAP: K_2CO_3 is 1:1.5.

3.3.5. *Effect of stirring rate on DMAP loading*

As shown in Figure 10, in the early stage of the reaction, the rate of loading reaction increased significantly when the stirring speed was gradually increased, which was because the loading of DMAP increased in the initial stage of the reaction as the moving rate increased and the mass transfer resistance decreased continuously. When the moving rate was 600 rpm, the loading reached the maximum value of 5.17 mmol/g. After that, the loading almost did not change when the moving rate increased. After that, there was practically no change in the loading when the stirring rate was increased. Therefore, when the stirring speed is slow, the mass transfer resistance hinders the loading of DMAP, and with the increase in stirring rate, the mass transfer resistance is gradually overcome. Still, the loading no longer increases after the mass transfer resistance decreases to a certain level. Therefore, 600 rpm is the best stirring rate for the reaction system.
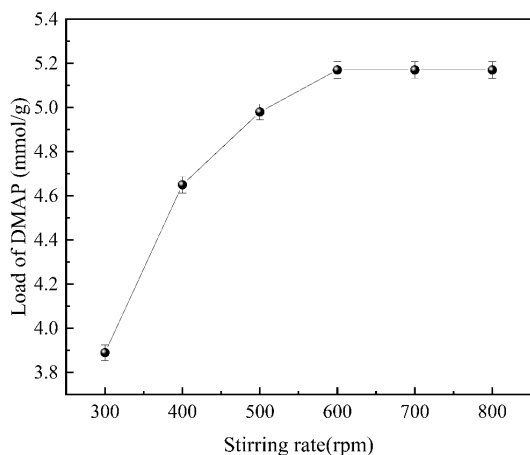
Figure 10. The effect of stirring rate on DMAP loading.

Figure 11. The Different degree of branching supported DMAP catalyzed acetylation reaction.

3.4. *Study of the reactivity of loaded DMAP with different branching levels*

Three catalysts with different branching degrees were applied to prepare vitamin E acetate. After the reaction, the conversion of vitamin E acetate by relevant calculations is shown in Figure 11. At the beginning of the reaction, the amount of vitamin E acetate gradually increased with the extension of time under the catalysis of the three catalysts. When the time was extended to 12 h, the amount of vitamin E acetate produced ceased to change. After the reaction was terminated and the sample was analyzed, the catalytic activity of the hyperbranched loaded catalyst was calculated to be the highest, 24.97 mmol/h·g. The catalytic activity of the grafted loaded catalyst was 15.99 mmol/h·g catalysts and 2.77 mmol/h·g for the non-branched loaded motivation, which indicated that the catalytic activity of the hyperbranched loaded catalyst was the highest.

3.5. *Exploration of the stability of loaded DMAPs with different branching levels*

In recent years, the recovery and recycling of catalysts have not only reduced pollution to the environment, in line with the green concept advocated by the state. Moreover, it dramatically reduces the cost of enterprises, which is beneficial to the long-term stable development of enterprises. Therefore,
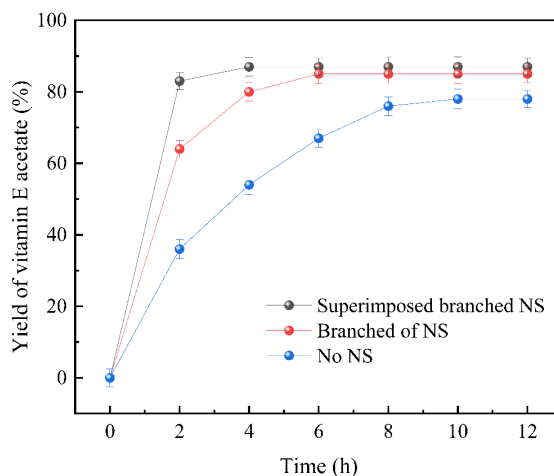
the recovery and recycling of catalysts have become one of the most popular research topics in this field. In this paper, the used target catalysts were recovered after the reaction and reused in a new acylation reaction according to the defined standard procedure. After the reaction, the sample spot plates obtained by sampling before and after the reaction were used to calculate the conversion of vitamin E acetate, and the results are shown in Figure 12. After ten recycling cycles, the three catalysts with different branching degrees had viability retention rates greater than 94.9%. Also, it can be seen from this figure that the catalytic activity of the hyperbranched loaded DMAP is the highest, which further indicates that the stability of the hyperbranched loaded DMAP synthesized in this thesis is excellent.

3.6. *Synthetic mechanisms and routes of vitamin E succinate*

Immobilized DMAP or free DMAP prepared in this thesis was used as a catalyst to react vitamin E with succinic anhydride as a reaction substrate to produce vitamin E succinate. This reaction type belongs to the catalytic acylation reaction of DMAP to vitamin E, that is, to alcohols, so the mechanism [27] of the acylation reaction of vitamin E and the synthesis route is shown in Scheme 1. Firstly, the pyridine nitrogen atom of DMAP attacks the electrophilic
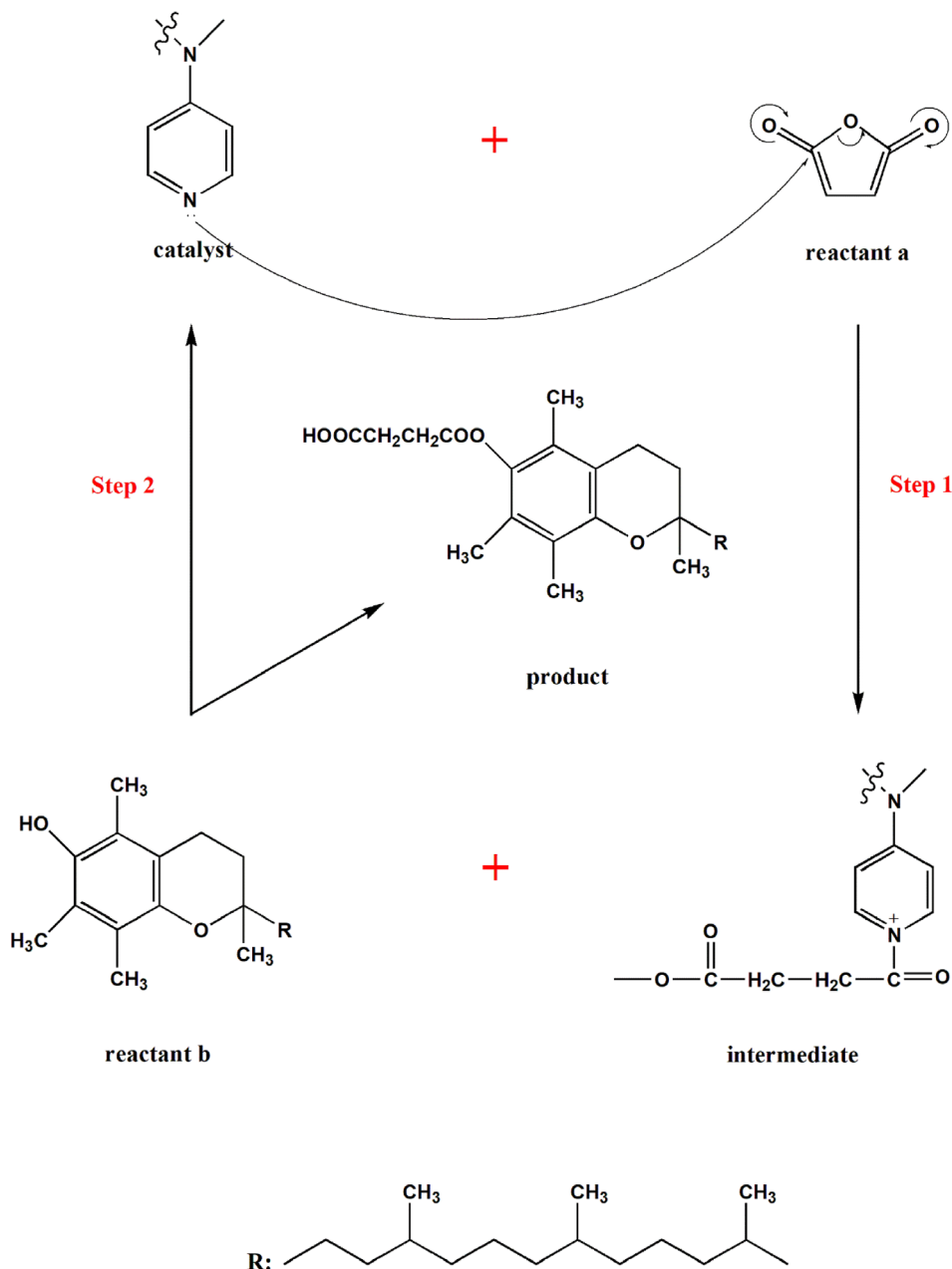
Scheme 1. Catalytic acetylation of vitamin E on DMAP; reactant a: succinic anhydride, reactant b: vitamin E, catalyst: free DMAP/branched DMAP/hyperbranched DMAP, product: vitamin E succinate.

carbonyl carbon of succinic anhydride to form 1-butanol-4-dimethylaminopyridine salt, which is the intermediate in Figure 1. Then the hydroxyl oxygen atom on vitamin E attacks the butyryl carbon atom connected with pyridine on the intermediate. Then the butyrate ion generated in the first step immediately seizes the hydrogen of the hydroxyl group on vitamin E to promote a positive reaction. The oxygen negative squeezes out the pyridine to obtain the target product, vitamin E succinate while regenerating a DMAP, followed by the next cycle.
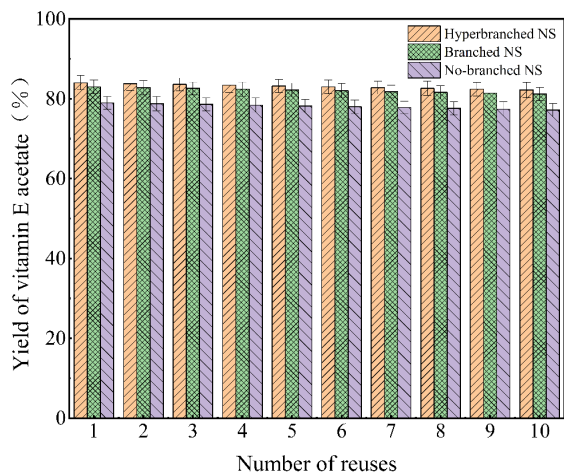
Figure 12. The recycling of catalysts with different degrees of branching.
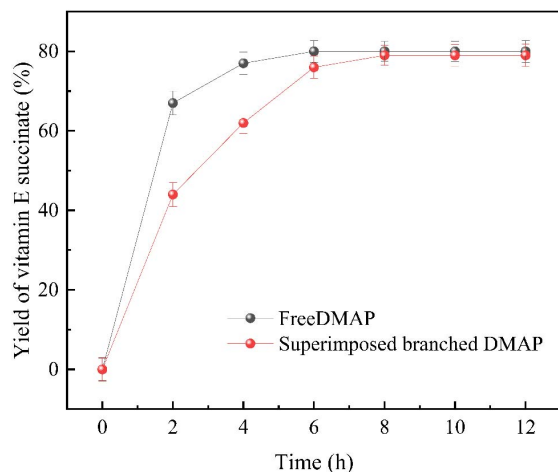

Figure 13. Hyperbranched supported DMAP catalyzed the acylation of vitamin E with succinic anhydride.

3.7. *Synthesis of vitamin E succinate*

In this paper, the hyperbranched loaded DMAP catalyst was applied to the synthesis reaction of vitamin E succinate, and the conversion of vitamin E was calculated after the reaction was completed, as shown in Figure 13. The catalytic activity of the free DMAP catalyst was 35.8 mmol/h·g, while the catalytic activity of the hyperbranched loaded DMAP catalyst was 19.5 mmol/h·g. The catalytic activity of the hyperbranched loaded DMAP catalyst was slightly lower than that of the free DMAP catalyst. The catalytic

activity of the latter was 1.9 times higher than that of the former 1.9 times. Compared with free DMAP, the activity of the hyperbranched-loaded DMAP was slightly lower. The reason for this is that the mass transfer resistance becomes larger after loading, so the activity of the hyperbranched loaded DMAP is lower than that of the free DMAP. However, after considering many factors, such as recycling of the catalysts in the reaction system, environmental protection, and the actual cost of industrial production, it was finally determined that the catalytic effect of hyperbranched loaded DMAP was the best. Hence, preparing hyperbranched-loaded DMAP catalysts has a broad application prospect.

4. Conclusion

In this paper, sorbitol was used as the grafting agent and nano-silica as the optimal carrier to investigate the effect of amplifying the surface hydroxyl group of the carrier to increase the loading of DMAP by hyper-grafting technique. After grafting the sorbitol onto the nano-silica, the surface hydroxyl content reached 8.89 mmol/g. Then the loading amount was 5.17 mmol/g after chloroalkylation conversion and N-alkylation loading of DMAP with nano silica as the carrier by sorbitol hyperbranched loading. Meanwhile, the prepared hyperbranched loaded DMAP catalyst was applied to the acylation-indicating reaction of vitamin E and acetic anhydride, and its activity and stability were evaluated and investigated. In addition, the super branched loaded DMAP catalyst was applied to the acylation reaction of vitamin E and succinic anhydride, and vitamin E succinate was successfully synthesized. In summary, the hyperbranched-loaded DMAP catalysts were successfully prepared while showing excellent chemical stability and outstanding catalytic performance.

Conflict of interest

No potential conflict of interest was reported by the authors.

Funding

References

[1] R. Murugan, E. Scriven, *Aldrichimica Acta*, 2003, **36**, 21-27.

[2] Scriven, F. V. Eric, *Chem. Soc. Rev.*, 1983, **12**, 129-161.

[3] S. Khajeh, F. Panahi, M. Nouri Sefat, A. Khalafi-Nezhad, *RSC Adv.*, 2016, **6**, 92316-92324.

[4] M. Puanngam, F. Unob, *J. Hazard. Mater.*, 2008, **154**, 578-587.

[5] A. Sunder, J. Heinemann, H. Frey, *Chemistry*, 2015, **6**, 2499-2506.

[6] D. Hölter, A. Burgath, H. Frey, *Acta Polym.*, 2010, **48**, 30-35.

[7] R. Hanselmann, H. Dirk, H. Frey, *Macromolecules*, 1998, **31**, 3790-3801.

[8] M. Seiler, C. Jork, A. Kavarnou, W. Arlt, R. Hirsch, *AIChE J.*, 2004, **19**, 2439-2454.

[9] L. Liang, L. Qiu, *Int. J. Pharm.*, 2021, **600**, article no. 120457.

[10] L. Liang, Y. Peng, L. Qiu, *J. Control. Release*, 2021, **337**, 117-126.

[11] X. T. Chen, J. X. Gu, L. Sun, W. Y. Li, L. L. Guo, Z. Y. Gu, L. T. Wang, Y. Zhang, W. W. Zhang, B. Q. Han, J. Chang, *Bioact. Mater.*, 2021, **6**, 3025-3032.

[12] T. A. Jacinto, C. F. Rodrigues, A. F. Moreira, S. P. Miguel, I. J. Correia, *Colloids Surf. B: Biointerfaces*, 2020, **188**, 110778-110788.

[13] B. K. Murray, B. Brown, P. M. Scherer, D. P. Tomer, K. L. O'Neill, *Nutr. Res.*, 2006, **26**, 186-192.

[14] E. A. Hassoun, D. Bagchi, M. Bagchi, S. J. Stohs, *Free Radic. Biol. Med.*, 1995, **18**, 577-590.

[15] Z. P. Evans, B. S. Mandavilli, J. D. Ellett, D. Rodwell, M. W. Fariss, R. N. Fiorini, R. G. Schnellmann, M. G. Schmidt, K. Chavin, *Transplant. Proc.*, 2009, **41**, 4094-4105.

[16] Y. J. Suzuki, L. Packer, *Biochem. Biophys. Res. Commun.*, 1993, **193**, 277-283.

[17] X. Huang, Z. Zhang, J. Li, Y. Zhao, X. Zhang, K. Wu, *Cancer Lett.*, 2010, **296**, 123-131.

[18] C. Y. Cao, X. L. Zhao, D. F. Tian, *Progr. Modern Biomed.*, 2009, **9**, 1673-1683.

[19] C. R. Hu, X. Zhao, Q. Y. Zhang, *China Fats Oils*, 2005, **30**, 42-45.

[20] Y. F. Ji, Y. B. Wang, *Chinese J. Pharma. Ind.*, 1996, **27**, 2-4.

[21] D. Chen, B. L. Li, B. Li, X. L. Zhang, L. H. Wei, W. W. Zheng, *Green Process. Synth.*, 2019, **1**, 667-676.

[22] M. Lei, Y. Wang, H. Zhao, Q. J. Peng, *Chem. Prog.*, 2012, **31**, 90-96.

[23] A. Klapars, S. L. Buchwald, *J. Am. Chem. Soc.*, 2003, **124**, 14844-14845.

[24] A. N. Kursunlu, E. Guler, H. Dumrul, O. Kocyigit, I. H. Gubbuk, *Appl. Surf. Sci.*, 2009, **255**, 8798-8803.

[25] Y. L. Wang, Z. J. Wan, J. Luo, *Org. Chem.*, 2019, **2**, 521-527.

[26] Z. He, Y. Wang, T. Zhao, Z. Ye, H. Huang, *Anal. Methods*, 2014, **6**, 4257-4261.

[27] W. Zhang, H. L. Fu, H. Jiang, Q. Fu, W. Tang, F. Zhou, *Heilongjiang Anim. Husb. Vet. Med.*, 2012, **1**, 4-9.